Electronic Supplementary Information (ESI)

Novel oxacalix[2]arene[2]triazines with thermally active delayed fluorescence and aggregation-induced emission properties

Yin-Feng Wang,[a] Hai-Yan Lu,[a,*] Yi-Fan Sheng,[a] Meng Li[b] and Chuan-Feng Chen[a,b,*]

[a]*University of Chinese Academy of Sciences, Beijing 100049, China. E-mail: haiyanlu@ucas.ac.cn*

[b]*Beijing National Laboratory for Molecular Sciences, CAS Key Laboratory of Molecular Recognition and Function, Institute of Chemistry, Chinese Academy of Sciences, Beijing 100190, China. E-mail: cchen@iccas.ac.cn*

Contents

1. General information

All the reagents were purchased from commercial sources and used without further purification. ^{1}H and ^{13}C NMR spectra were recorded on AVIII 500 MHz NMR spectrometers in $CDCl_3$ solutions. High resolution mass spectra were measured on a Thermo Fisher® Exactive high resolution LC-MS spectrometer. The calculation was carried out with the Gaussian 09 software package. Geometry optimizations were conducted under the M06-2X/6-31g(d) level of theory. Crystal structures were solved with direct methods and refined with a full-matrix least-squares technique, using the SHELXS software package. Cyclic voltammetry was performed using a CHI600A analyzer with a scan rate of 100 mV/s at room temperature to investigate the oxidation potentials. A conventional three electrode cell was used as electrolytic cell with a glassy carbon working electrode, an Ag/Ag^{+} (0.01 M $AgNO_3$) as the reference electrode, and Pt wire as the counter electrode. The oxidation potential was measured in CH_2Cl_2 with 0.1 M of tetra-n-butylammonium hexafluorophosphate ($n\text{-}Bu_4NPF_6$) as a supporting electrolyte. Fc/Fc^{+} (0.15 eV against $Ag/AgNO_3$) used as internal standard for calibrating the reference electrode.

UV–Vis spectra were recorded on PerkinElmer® UV/Vis/NIR spectrometer (Lambda 950), and the fluorescence spectra were recorded on HITACHI® F-7000 Fluorescence Spectrometer at room temperature. The transient photoluminance decay characteristics and temperature dependence experiments and absolute PL quantum yield were measured on an Edinburgh Instruments FLS980 spectrometer.

2. Synthetic procedures and characterized data

Compounds **1**, **2**, **3**, **4** and **OC2A2T** were synthesized according to the literatures.[S1-S4]

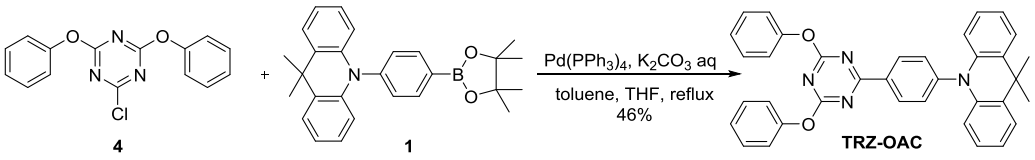

Synthesis of compound **TRZ-OAC**: Compound **1** (1.7 g, 4.0 mmol), compound **4** (599.4 mg, 2.0 mmol), $Pd(PPh_3)_4$ (69.4 mg, 0.06 mmol), 2 M K_2CO_3 solution (8 mL),

THF (6 mL) and toluene (16 mL) were added into a two neck flask. The mixture was refluxed under a dry argon atmosphere for 24 h. After cooling to room temperature, the reaction mixture was extracted with dichloromethane, washed with brine and dried over anhydrous Na_2SO_4. After the solvent was removed under reduced pressure, the residue was purified by column chromatography to give the target material as a green powder (504.7 mg, 46% yield). Mp: 114-116 °C. ^{1}H NMR (500 MHz, $CDCl_3$): δ 8.52 (d, *J* = 8.4 Hz, 2H), 7.48–7.38 (m, 8H), 7.31–7.24 (m, 6H), 6.99–6.90 (m, 4H), 6.28 (d, *J* = 7.4 Hz, 2H), 1.67 (s, 6H). ^{13}C NMR (126 MHz, $CDCl_3$): δ 175.1, 173.0, 151.8, 146.1, 140.4, 134.1, 131.8, 131.1, 130.6, 129.5, 126.3, 126.0, 125.2, 121.6, 121.0, 114.3, 36.0, 31.0. HR-MS (APCI): *m/z* calcd for $C_{36}H_{28}N_4O_2^+$ $[M + H]^+$ 548.2212, found 549.2281.

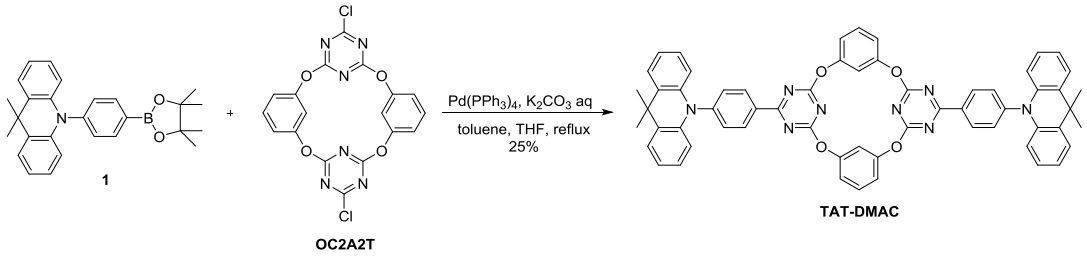

Synthesis of **TAT-DMAC**: Mp: >300 °C. Compound **1** (1.2 g, 3.0 mmol), compound **8** (443.2 mg, 1.0 mmol), $Pd(PPh_3)_4$ (34.7 mg, 0.03 mmol), 2 M K_2CO_3 solution (12 mL), THF (9 mL) and toluene (24 mL) were added into a two neck flask. The mixture was refluxed under a dry argon atmosphere for 24 h. After cooling to room temperature, the reaction mixture was extracted with dichloromethane, washed with brine and dried over anhydrous Na_2SO_4. After the solvent was removed under reduced pressure, the residue was purified by column chromatography to give the target material as a green powder (235.1 mg, 25% yield). ^{1}H NMR (500 MHz, $CDCl_3$): δ 8.84 (d, *J* = 8.2 Hz, 4H), 7.56 (d, *J* = 8.2 Hz, 4H), 7.49 (d, *J* = 7.5 Hz, 4H), 7.35 (t, *J* = 8.1 Hz, 2H), 7.06–6.94 (m, 12H), 6.86 (t, *J* = 2.1 Hz, 2H), 6.38 (d, *J* = 7.8 Hz, 4H), 1.71 (s, 12H). ^{13}C NMR (126 MHz, $CDCl_3$): δ 176.4, 173.1, 152.1, 146.5, 140.5, 133.9, 131.9, 131.2, 130.7, 130.5, 126.4, 125.4, 121.1, 119.4, 116.6, 114.4, 36.1, 31.1. HR-MS (APCI): *m/z* calcd for $C_{60}H_{45}O_4N_8$ $[M]^+$ 941.3558, found 941.3550.

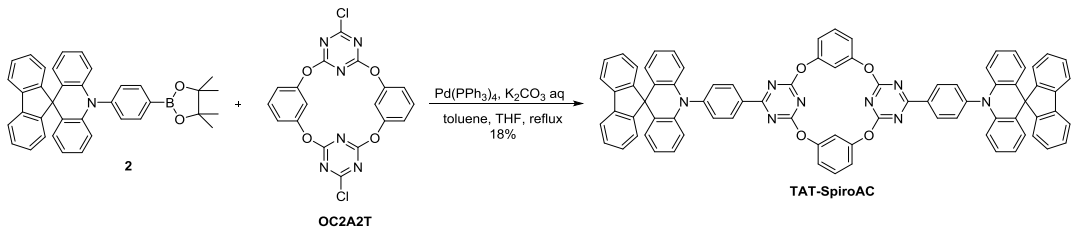

Synthesis of **TAT-SpiroAC**: Mp: >300 °C. A procedure similar to that used for compound **TAT-DMAC** was followed but with compound **2** (1.6 g, 3.0 mmol) instead of compound **1**. The crude product was purified by column chromatography on silica gel to obtain a green powder (639.9 mg, 18% yield). ^{1}H NMR (500 MHz, $CDCl_3$): δ 8.94 (d, *J* = 8.2 Hz, 4H), 7.82 (d, *J* = 7.5 Hz, 4H), 7.72 (d, *J* = 8.3 Hz, 4H), 7.44 (d, *J* = 7.5 Hz, 4H), 7.42–7.35 (m, 6H), 7.29 (d, *J* = 7.4 Hz, 4H), 7.01 (d, *J* = 8.1 Hz, 4H), 6.95 (t, *J* = 7.6 Hz, 4H), 6.90 (s, 2H), 6.60 (t, *J* = 7.4 Hz, 4H), 6.47–6.38 (m, 8H). ^{13}C NMR (126 MHz, $CDCl_3$): δ 176.3, 173.2, 156.5, 152.1, 146.1, 140.8, 139.2, 134.5, 132.1, 131.9, 130.5, 128.4, 128.0, 127.6, 127.3, 125.8, 125.0, 120.9, 119.9, 119.5, 116.6, 114.5, 56.8. HR-MS (APCI): *m/z* calcd for $C_{80}H_{48}O_4N_8$ $[M]^+$1185.3871, found 1185.3875.

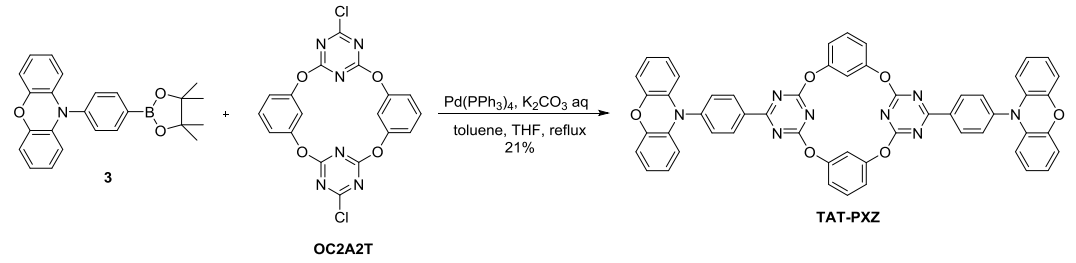

Synthesis of **TAT-PXZ**: Mp: >300 °C. A procedure similar to that used for compound **TAT-DMAC** was followed but with compound **3** (1.2 g, 3.0 mmol) instead of compound **1**. The crude product was purified by column chromatography on silica gel to obtain an orange powder (560.1 mg, 21% yield). ^{1}H NMR (500 MHz, $CDCl_3$): δ 8.80 (d, *J* = 8.4 Hz, 4H), 7.55 (d, *J* = 8.5 Hz, 4H), 7.34 (t, *J* = 8.2 Hz, 2H), 6.97 (dd, *J* = 8.2, 2.2 Hz, 4H), 6.84 (t, *J* = 2.1 Hz, 2H), 6.78–6.57 (m, 12H), 6.02 (d, *J* = 7.9 Hz, 4H). ^{13}C NMR (126 MHz, $CDCl_3$): δ 176.1, 173.1, 152.1, 144.0, 134.3, 133.7, 132.0, 131.1, 130.5, 123.3, 121.8, 119.4, 116.6, 115.7, 113.4. HR-MS (APCI): *m/z* calcd for $C_{54}H_{32}O_6N_8$ $[M]^+$ 889.2518, found 889.2513.

3. Single crystal structure and theoretical calculation

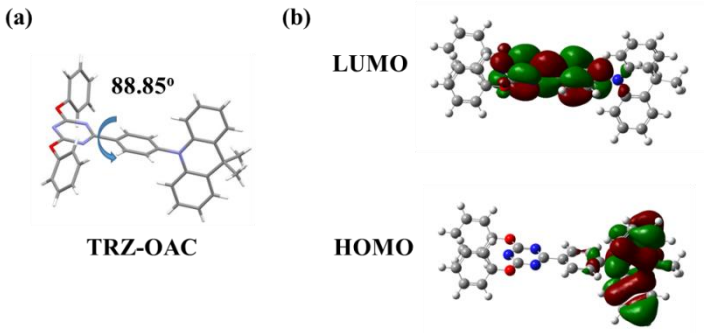

Fig. S1. (a) Crystal structure of **TRZ-OAC**. (b) Calculated spatial distributions of the HOMO/LUMO of **TRZ-OAC**.

4. Electrochemical properties

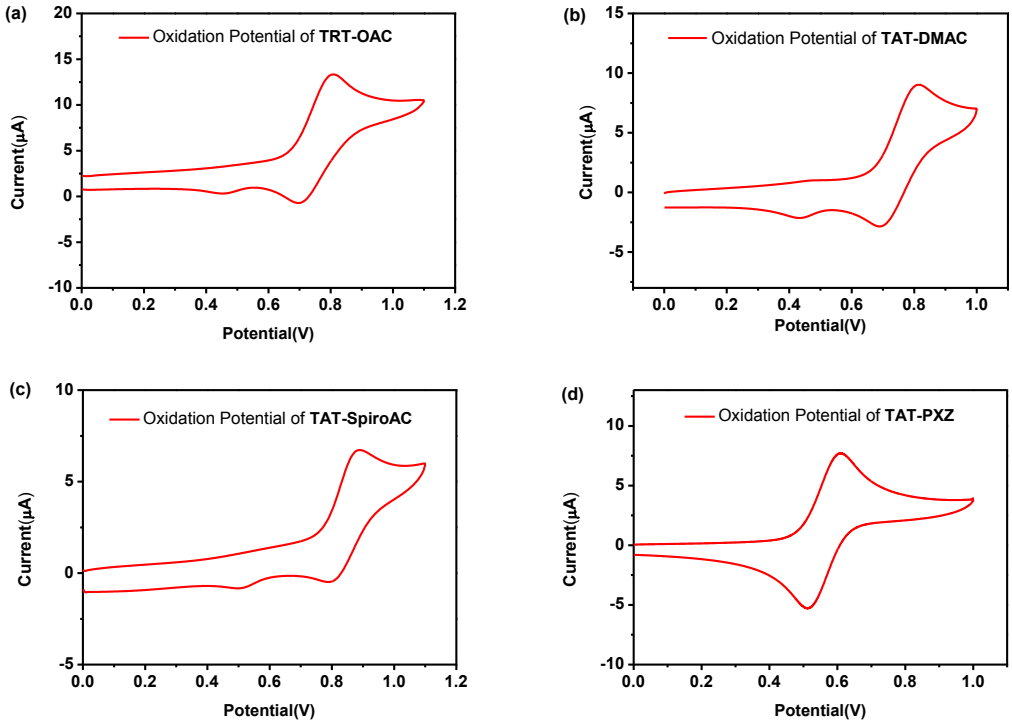

Fig. S2. Cyclic voltammetry of **TRZ-OAC**, **TAT-DMAC**, **TAT-SpiroAC** and **TAT-PXZ** with ferrocene as internal standard. Oxidation potential of (a) **TRZ-OAC**, (b) **TAT-DMAC**, (c) **TAT-SpiroAC** and (d) **TAT-PXZ**.

Table S1. The electrochemical properties of **TRZ-OAC**, **TAT-DMAC**, **TAT-SpiroAC** and **TAT-PXZ**.

	$E_{ox,onset}$ V	E_{HOMO} eV	E_{LUMO} eV	$E_{g,opt}$ eV
TRZ-OAC	0.67	-5.32	-2.64	2.68
TAT-DMAC	0.67	-5.32	-2.70	2.62
TAT-SpiroAC	0.77	-5.49	-2.72	2.70
TAT-PXZ	0.49	-5.41	-2.67	2.47

5. Photophysical properties

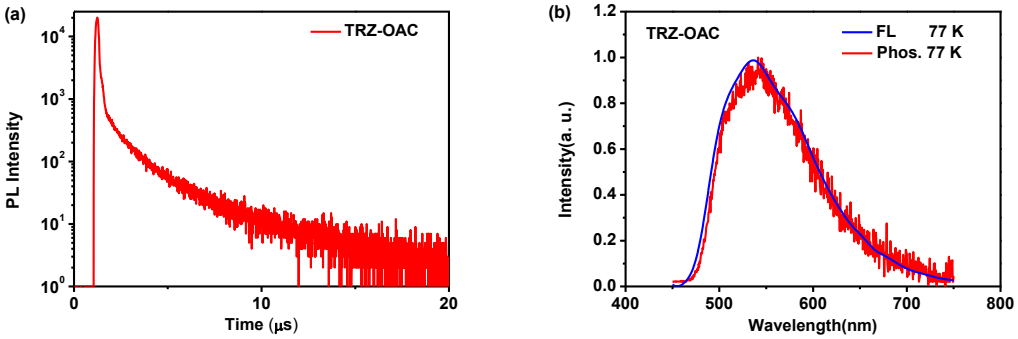

Fig. S3. (a) Transient PL spectra of **TRZ-OAC** in neat film at room temperature. (b) Normalized photoluminescence and phosphorescence spectra of **TRZ-OAC** in neat film at 77 K.

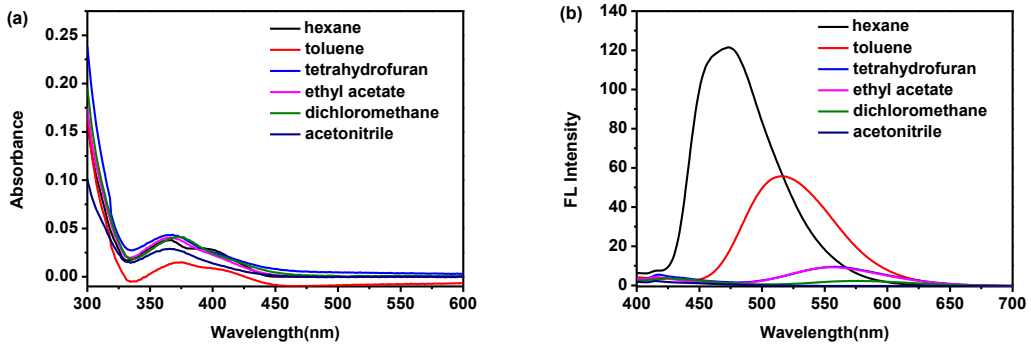

Fig. S4. (a) Absorption spectra, (b) fluorescence spectra of **TRZ-OAC** in different solvents at room temperature (c = 1.0 ×10^{-5} M).

Table S2. Absorption and emission characteristics of **TRZ-OAC** in different solvents at room temperature (c = 1.0 ×10^{-5} M).

solvent	λ_{abs} (nm)	λ_{em} (nm)
hexane	367	473
toluene	375	515
THF	368	557
ethyl acetate	366	554
dichloromethane	366	578
acetonitrile	366	N.D.

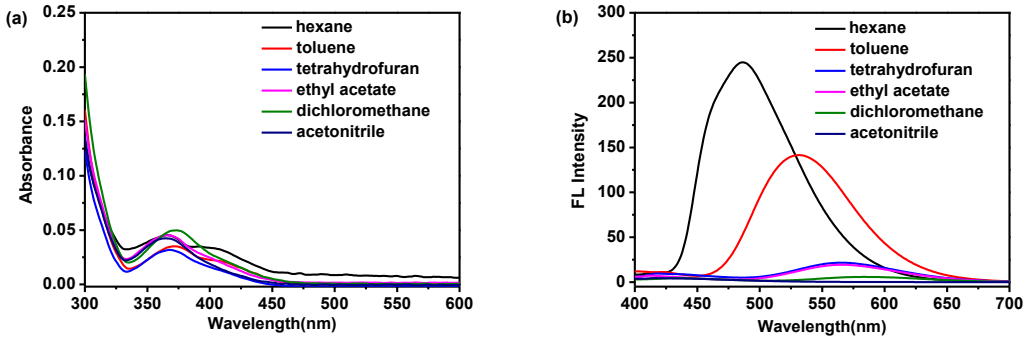

Fig. S5. (a) Absorption spectra, (b) fluorescence spectra of **TAT-DMAC** in different solvents at room temperature (c = 1.0 ×10^{-5} M).

Table S3. Absorption and emission characteristics of **TAT-DMAC** in different solvents at room temperature (c = 1.0 ×10^{-5} M).

solvent	λ_{abs} (nm)	λ_{em} (nm)
hexane	365	486
toluene	372	531
THF	367	565
ethyl acetate	366	565
dichloromethane	376	584
acetonitrile	365	N.D.

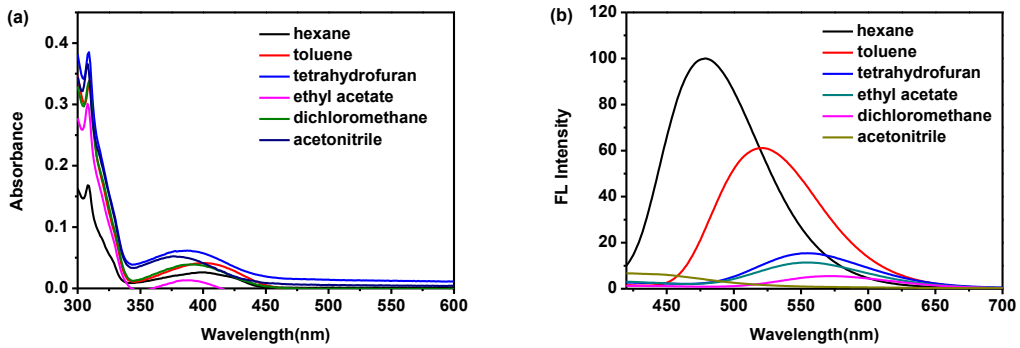

Fig. S6. (a) Absorption spectra, (b) fluorescence spectra of **TAT-SpiroAC** in different solvents at room temperature (c = 1.0 ×10^{-5} M).

Table S4. Absorption and emission characteristics of **TAT-SpiroAC** in different solvents at room temperature (c = 1.0 ×10^{-5} M).

solvent	λ_{abs} (nm)	λ_{em} (nm)
hexane	402	479
toluene	401	521
THF	387	555
ethyl acetate	389	554
dichloromethane	389	574
acetonitrile	376	N.D.

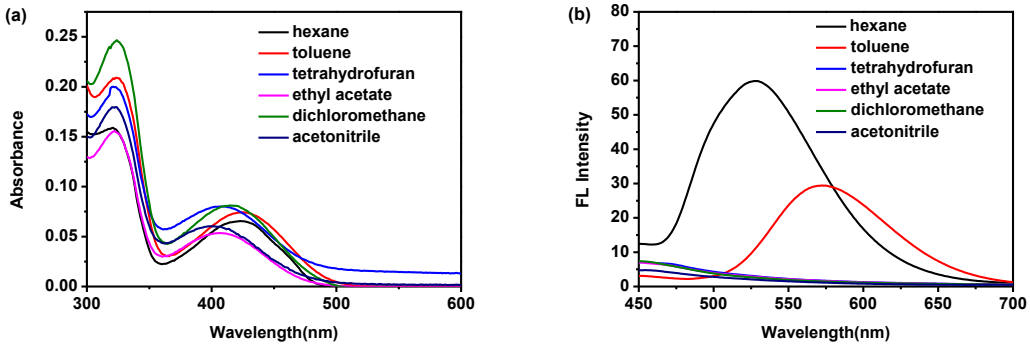

Fig. S7. (a) Absorption spectra, (b) fluorescence spectra of **TAT-PXZ** in different solvents at room temperature (c = 1.0 ×10^{-5} M).

Table S5. Absorption and emission characteristics of **TAT-PXZ** in different solvents at room temperature (c = 1.0 ×10^{-5} M).

solvent	λ_{abs} (nm)	λ_{em} (nm)
hexane	423	528
toluene	426	572
THF	409	N.D.
ethyl acetate	408	N.D.
dichloromethane	415	N.D.
acetonitrile	399	N.D.

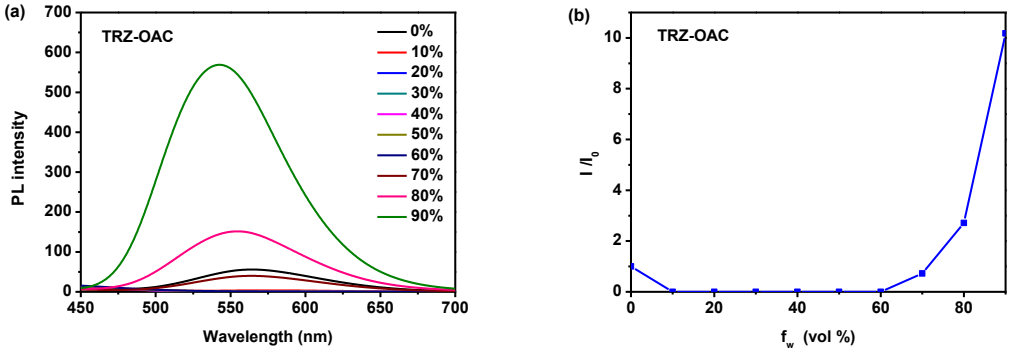

Fig. S8. (a) PL spectra of **TRZ-OAC** in THF/H_2O mixtures with different f_w. (b) Plots of the I/I_0 of the THF/H_2O mixtures of **TRZ-OAC**.

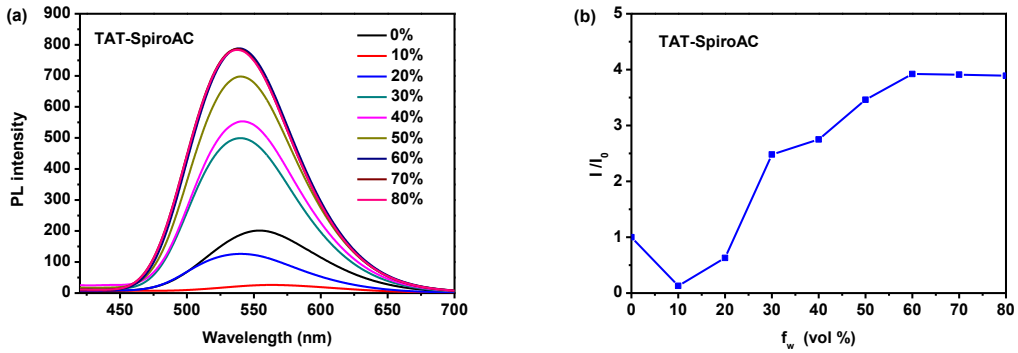

Fig. S9. (a) PL spectra of **TAT-SpiroAC** in THF/H_2O mixtures with different f_w. (b) Plots of the I/I_0 of the THF/H_2O mixtures of **TAT-SpiroAC**.

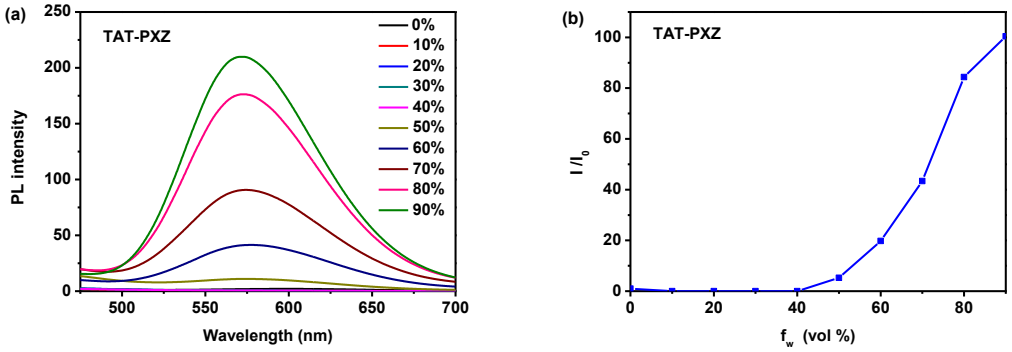

Fig. S10. (a) PL spectra of **TAT-PXZ** in THF/H_2O mixtures with different f_w. (b) Plots of the I/I_0 of the THF/H_2O mixtures of **TAT-PXZ**.

Table S6. PLQYs of **TRZ-OAC**, **TAT-DMAC**, **TAT-SpiroAC** and **TAT-PXZ** in thin film.

	TRZ-OAC	**TAT-DMAC**	**TAT-SpiroAC**	**TAT-PXZ**
atmosphere	47.2%	50.5%	48.7%	12.8%
vacuum	50.4%	65.0%	60.3%	16.8%

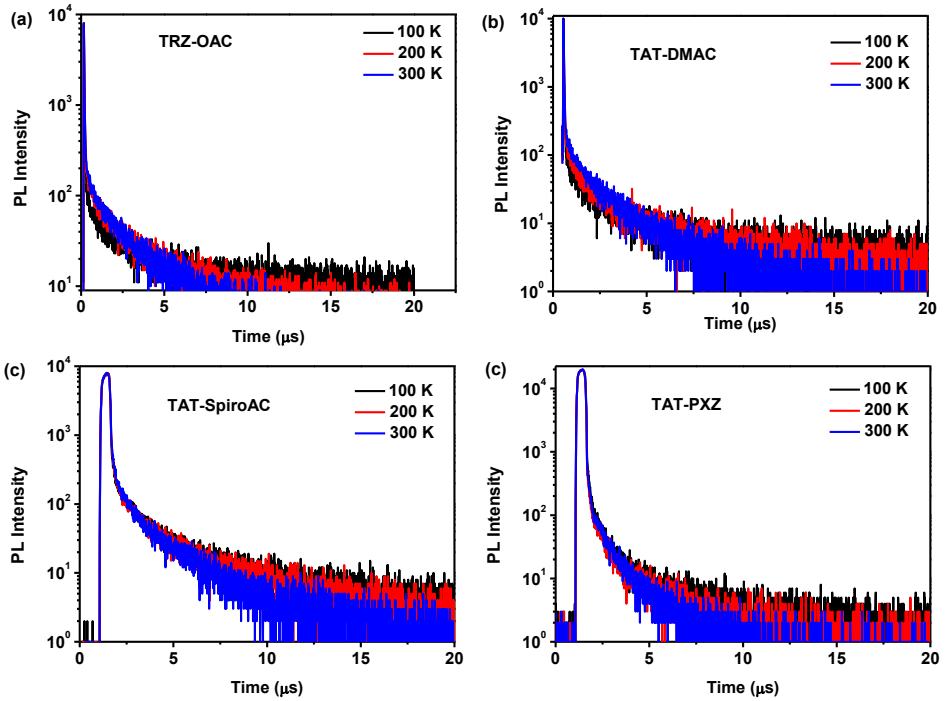

Fig. S11. Temperature-dependent transient PL decay spectra of **TRZ-OAC**, **TAT-DMAC**, **TAT-SpiroAC** and **TAT-PXZ** in neat film.

6. Copies of ^{1}H NMR and ^{13}C NMR spectra of new compounds

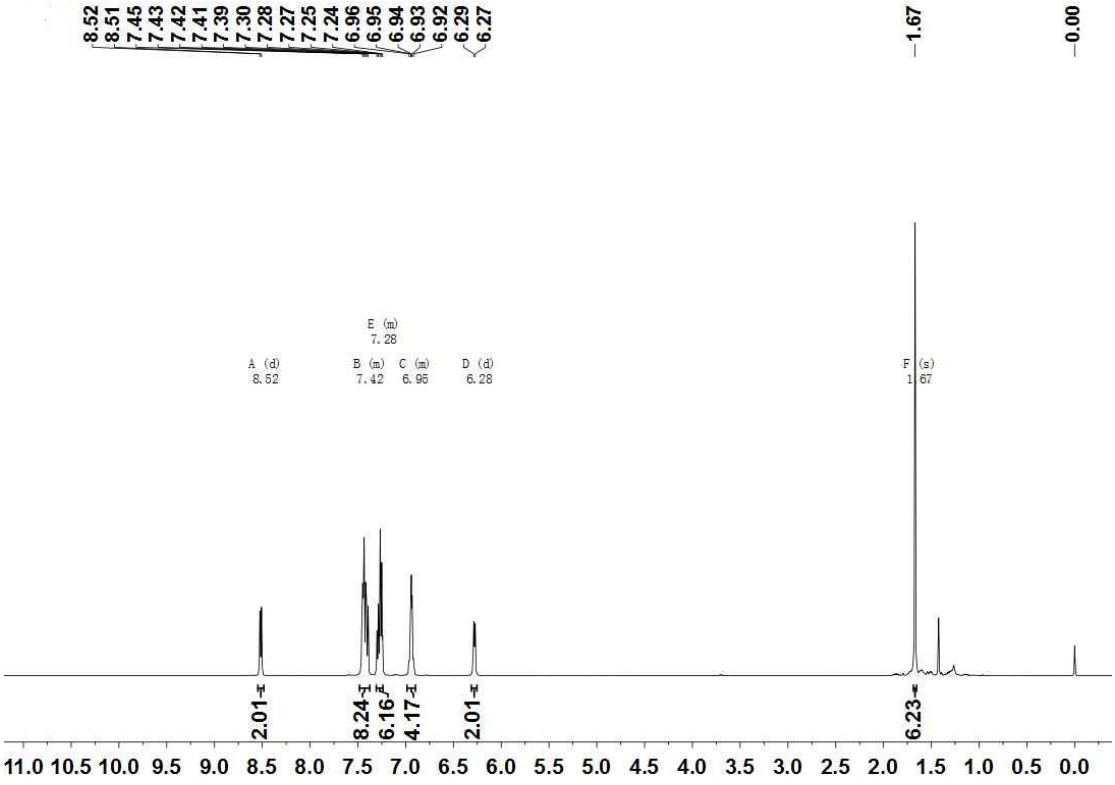

Fig. S12. ^{1}H NMR spectrum of **TRZ-OAC** in $CDCl_3$ (500 MHz, 298 K).

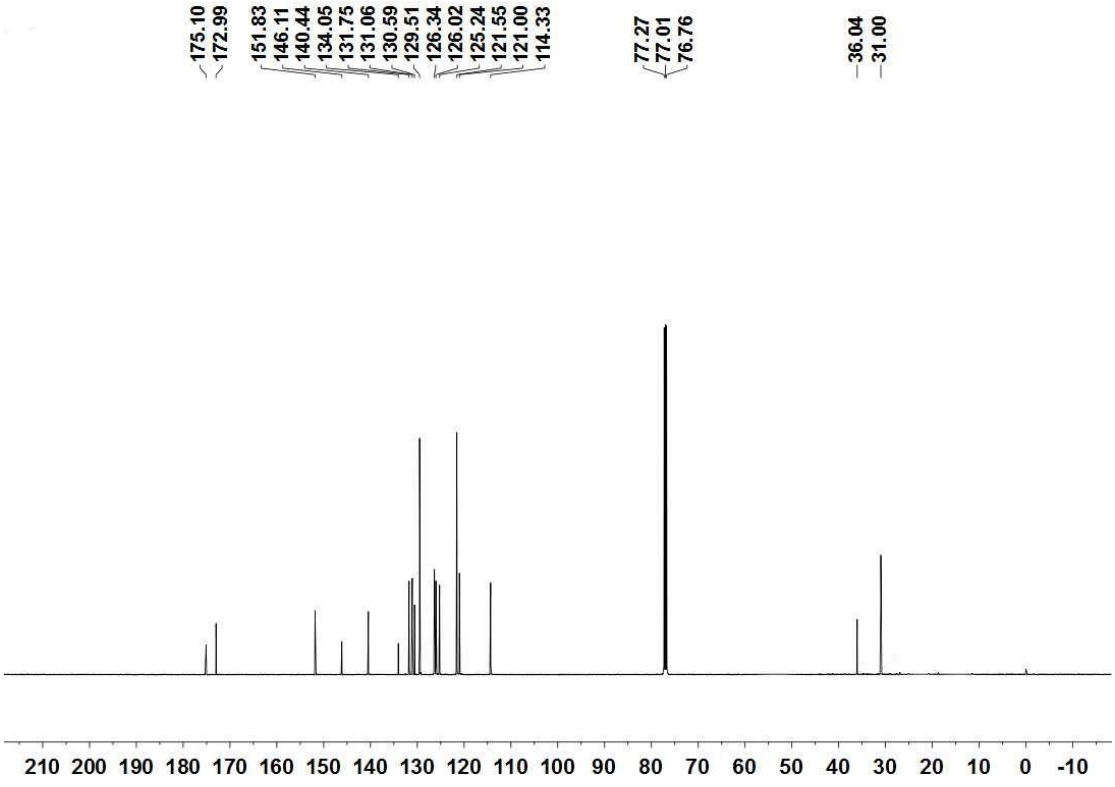

Fig. S13. ^{13}C NMR spectrum of **TRZ-OAC** in $CDCl_3$ (126 MHz, 298 K).

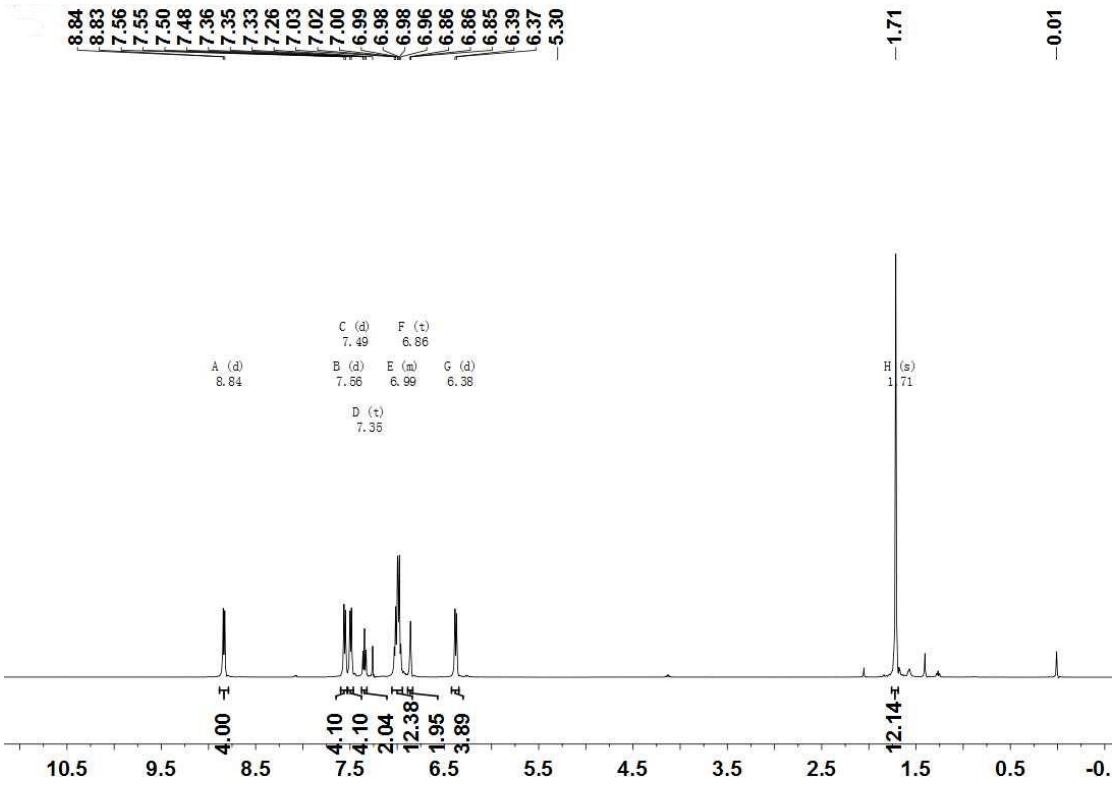

Fig. S14. ^{1}H NMR spectrum of **TAT-DMAC** in $CDCl_3$ (500 MHz, 298 K).

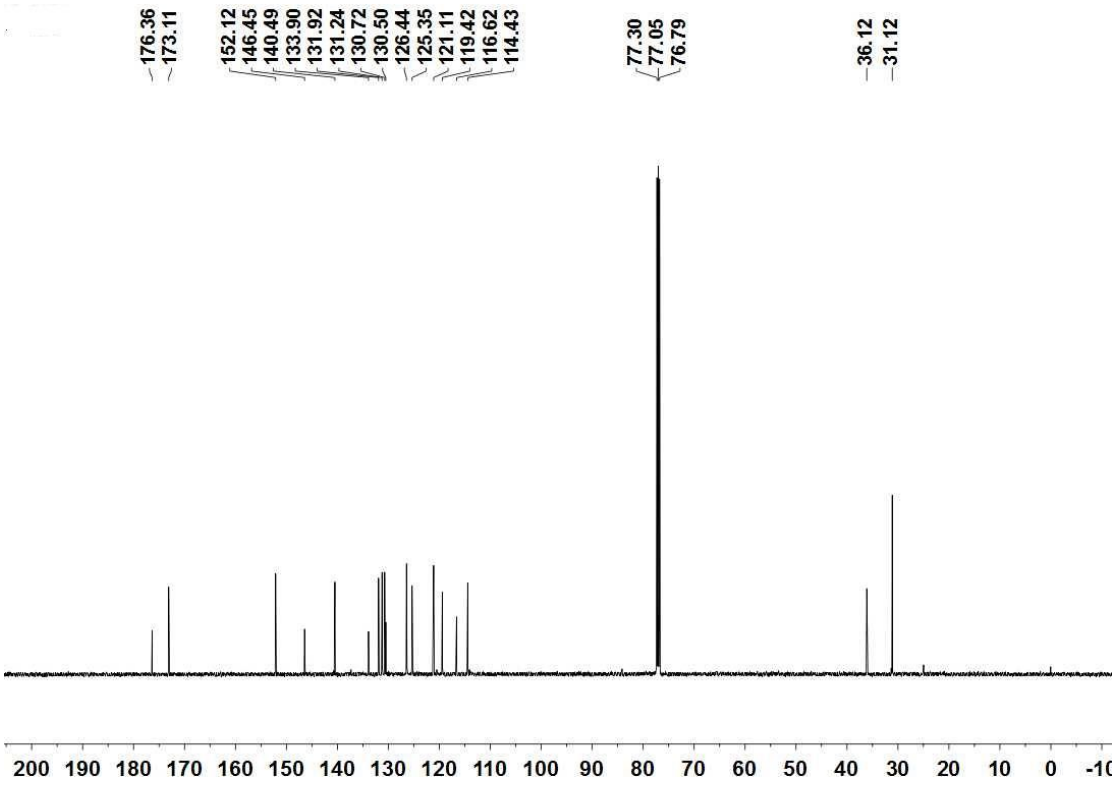

Fig. S15. ^{13}C NMR spectrum of **TAT-DMAC** in $CDCl_3$ (126 MHz, 298 K).

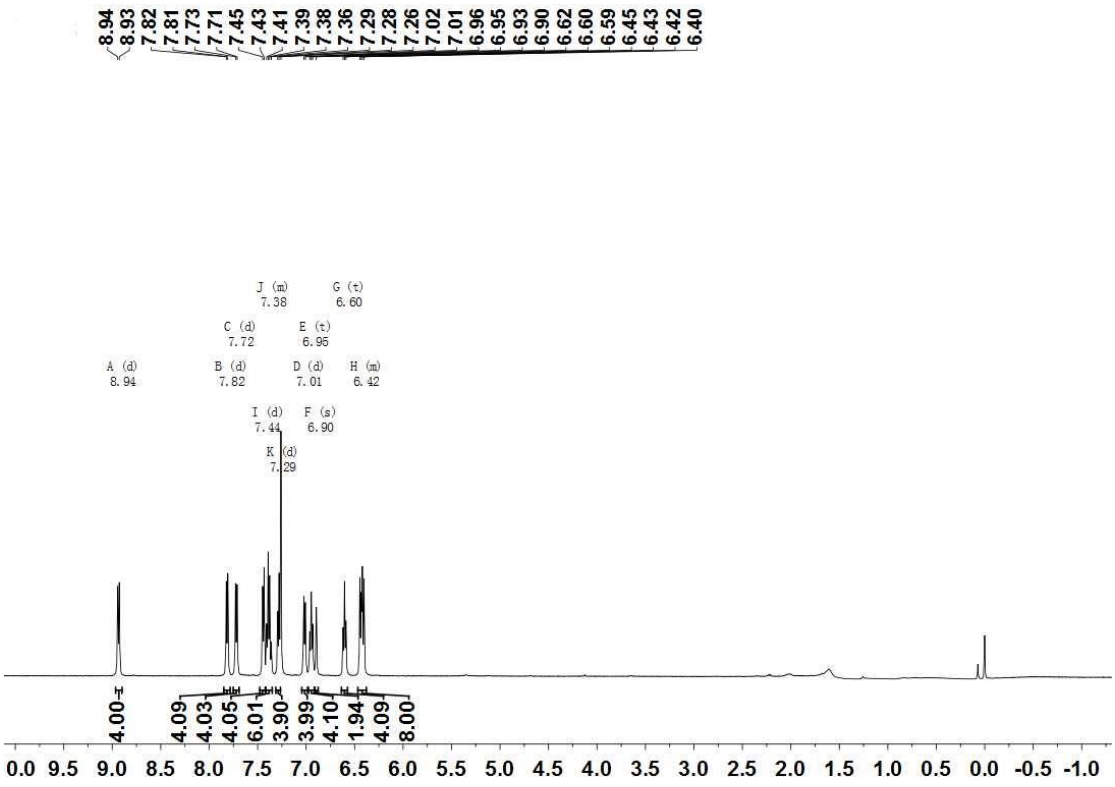

Fig. S16. ^{1}H NMR spectrum of **TAT-SpiroAC** in $CDCl_3$ (500 MHz, 298 K).

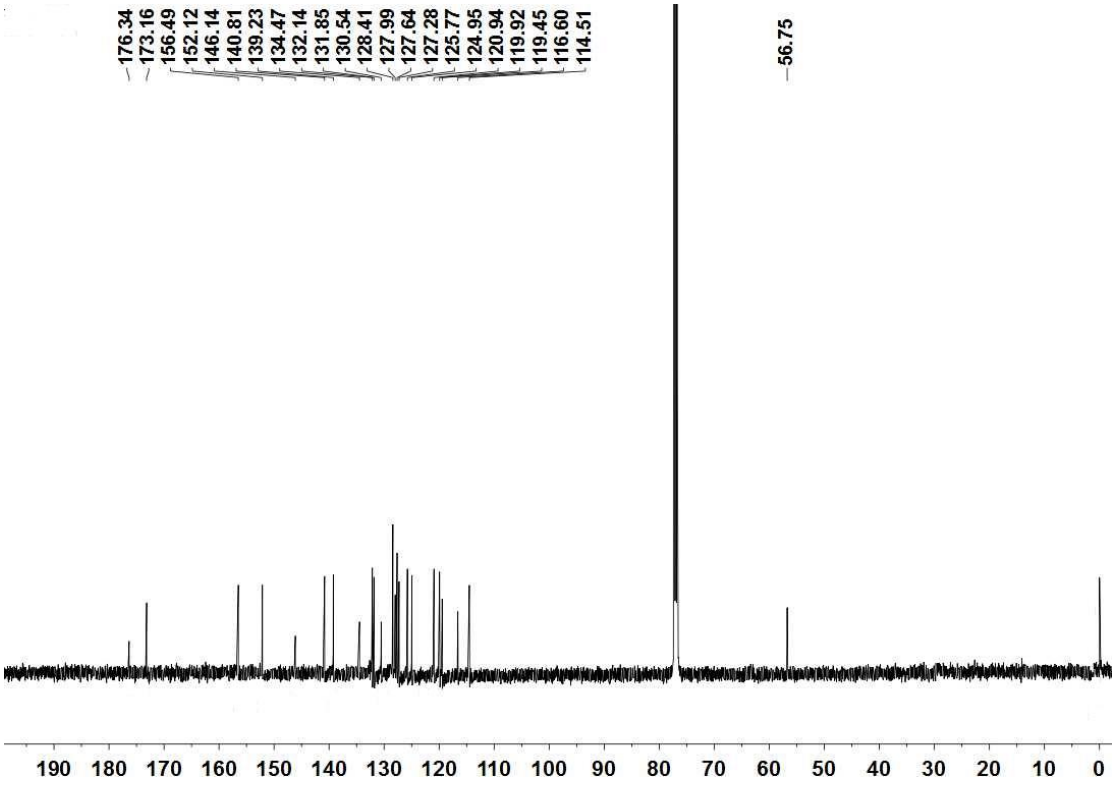

Fig. S17. ^{13}C NMR spectrum of **TAT-SpiroAC** in $CDCl_3$ (126 MHz, 298 K).

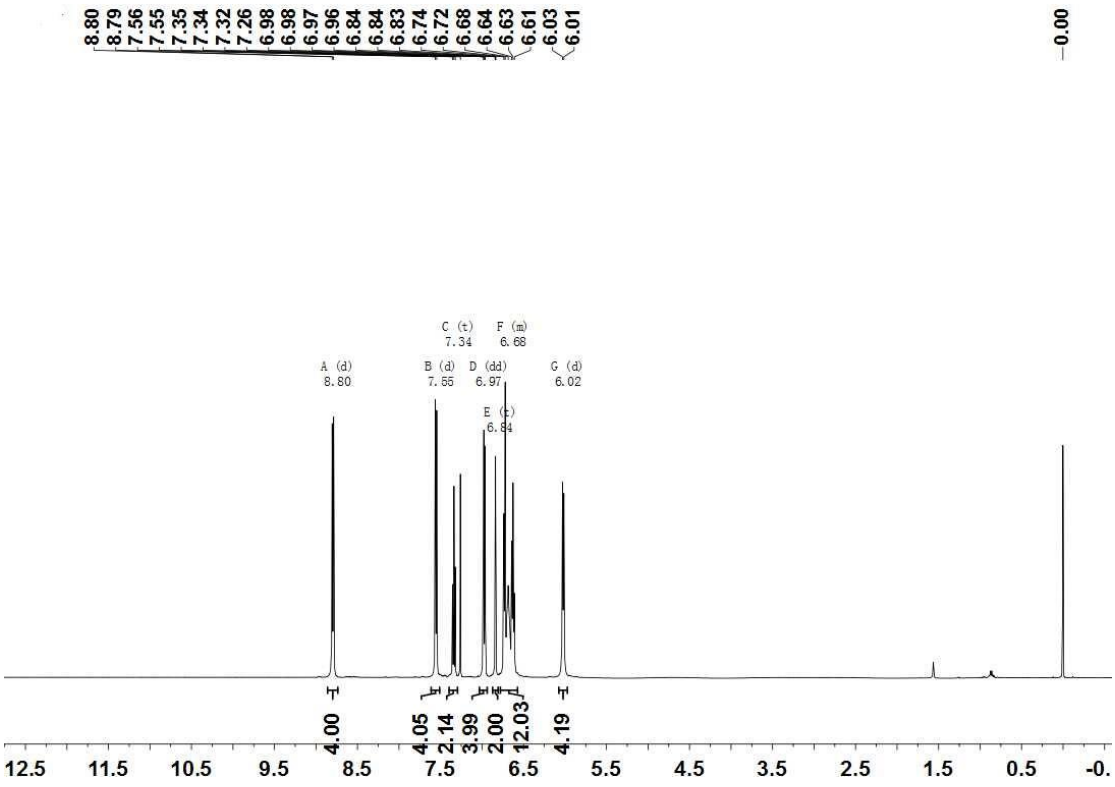

Fig. S18. ^{1}H NMR spectrum of **TAT-PXZ** in $CDCl_3$ (500 MHz, 298 K).

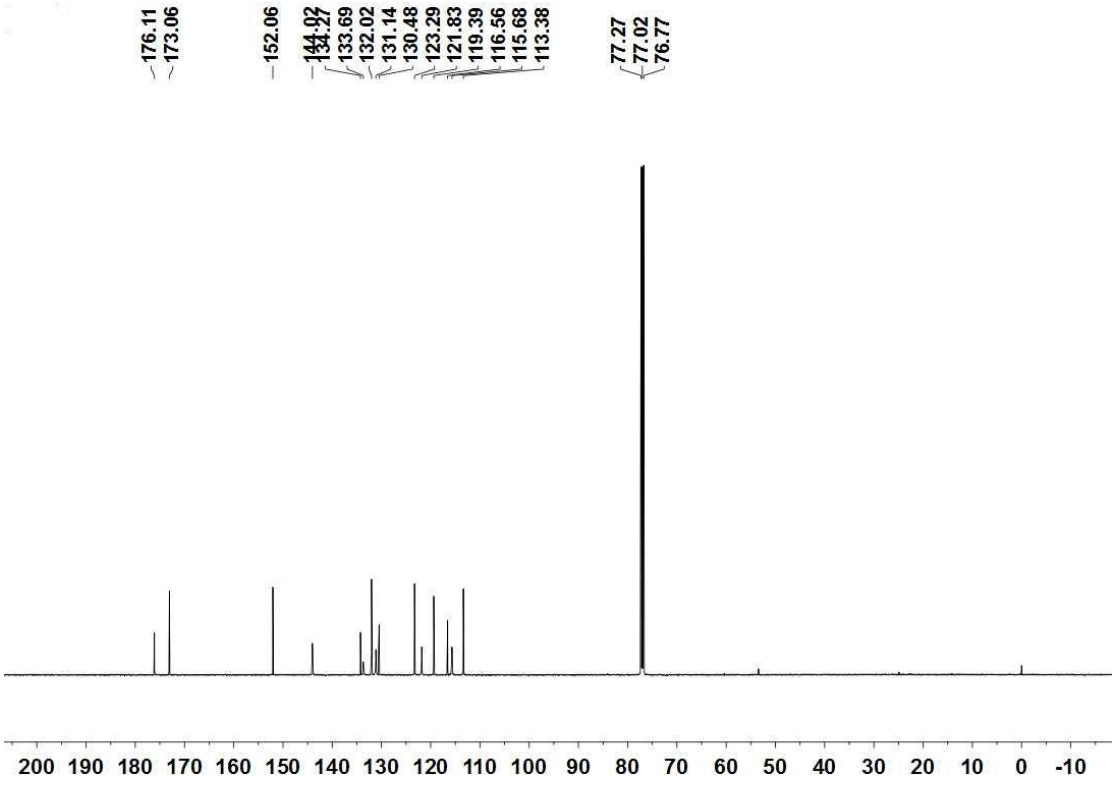

Fig. S19. ^{13}C NMR spectrum of **TAT-PXZ** in $CDCl_3$ (126 MHz, 298 K).

7. X-ray crystallographic data

Table S7. Single crystal data of compound **TRZ-OAC** (CCDC: 1922443).

Identification code	tx401	
Empirical formula	$C_{36}H_{28}N_4O_2$	
Formula weight	548.62	
Temperature	170.01(10) K	
Wavelength	1.54184 Å	
Crystal system	Orthorhombic	
Space group	P n n a	
Unit cell dimensions	a = 11.45750(10) Å	α= 90°.
	b = 10.69620(10) Å	β= 90°.
	c = 27.0458(2) Å	γ= 90°.
Volume	3314.51(5) $Å^3$	
Z	4	
Density (calculated)	1.099 Mg/m^3	
Absorption coefficient	0.550 mm^{-1}	
F(000)	1152	
Crystal size	0.355 x 0.345 x 0.324 mm^3	
Theta range for data collection	4.445 to 75.336 °.	
Index ranges	-12<=h<=13, -13<=k<=13,	
-33<=l<=33		
Reflections collected	30875	
Independent reflections	3289 [R(int) = 0.0223]	
Completeness to theta = 67.684 °	99.3 %	
Absorption correction	Semi-empirical from equivalents	
Max. and min. transmission	1.00000 and 0.64137	
Refinement method	Full-matrix least-squares on F^2	
Data / restraints / parameters	3289 / 0 / 194	
Goodness-of-fit on F^2	1.053	
Final R indices [I>2sigma(I)]	R1 = 0.0404, wR2 = 0.1154	
R indices (all data)	R1 = 0.0431, wR2 = 0.1217	
Extinction coefficient	n/a	
Largest diff. peak and hole	0.201 and -0.184 $e.Å^{-3}$	

Table S8. Single crystal data of compound **TAT-DMAC** (CCDC: 1922444).

Identification code	tx457_sq
Empirical formula	$C_{60}H_{44}N_8O_4$
Formula weight	941.03
Temperature/K	170.00(10)
Crystal system	monoclinic
Space group	$P2_1/c$
a/Å	9.64598(5)
b/Å	27.23322(15)
c/Å	18.74004(10)
α/°	90
β/°	101.9258(5)
γ/°	90
Volume/Å^3	4816.58(5)
Z	4
ρ_{calc}g/cm^3	1.298
μ/mm^{-1}	0.666
F(000)	1968.0
Crystal size/mm^3	0.257 × 0.213 × 0.15
Radiation	CuKα (λ = 1.54184)
2Θ range for data collection/°	5.81 to 151.012
Index ranges	$-11 \le h \le 12$, $-30 \le k \le 33$, $-23 \le l \le 23$
Reflections collected	34940
Independent reflections	9511 [R_{int} = 0.0195, R_{sigma} = 0.0167]
Data/restraints/parameters	9511/1/653
Goodness-of-fit on F^2	1.054
Final R indexes [I>=2σ (I)]	R_1 = 0.0466, wR_2 = 0.1306
Final R indexes [all data]	R_1 = 0.0510, wR_2 = 0.1355
Largest diff. peak/hole / e Å^{-3}	0.59/-0.21

Table S9. Single crystal data of compound **TAT-SpiroAC** (CCDC: 1922445).

Identification code	tx402a_sq
Empirical formula	$C_{80}H_{48}N_8O_4$
Formula weight	1185.26
Temperature	169.99(10) K
Wavelength	1.54178 Å
Crystal system	Monoclinic

Space group	P 1 21/n 1	
Unit cell dimensions	a = 14.9786(4) Å	α= 90°.
	b = 9.0590(2) Å	β= 94.208(2)°.
	c = 57.2212(11) Å	γ= 90°.
Volume	7743.5(3) $Å^3$	
Z	4	
Density (calculated)	1.017 Mg/m^3	
Absorption coefficient	0.507 mm^{-1}	
F(000)	2464	
Crystal size	0.245 x 0.034 x 0.023 mm^3	
Theta range for data collection	3.002 to 75.626 °.	
Index ranges	-17<=h<=18, -11<=k<=8, -71<=l<=71	
Reflections collected	52610	
Independent reflections	15105 [R(int) = 0.0615]	
Completeness to theta = 67.679 °	98.3 %	
Absorption correction	Semi-empirical from equivalents	
Max. and min. transmission	1.00000 and 0.69174	
Refinement method	Full-matrix least-squares on F^2	
Data / restraints / parameters	15105 / 0 / 829	
Goodness-of-fit on F^2	1.089	
Final R indices [I>2sigma(I)]	R1 = 0.0832, wR2 = 0.2327	
R indices (all data)	R1 = 0.0968, wR2 = 0.2421	
Extinction coefficient	n/a	
Largest diff. peak and hole	0.369 and -0.330 e.$Å^{-3}$	

Table S10. Single crystal data of compound **TAT-PXZ** (CCDC: 1922447).

Identification code	tx372b_sq	
Empirical formula	$C_{54}H_{32}N_8O_6$	
Formula weight	888.87	
Temperature	173(2) K	
Wavelength	1.54178 Å	
Crystal system	Monoclinic	
Space group	P 1 2/c 1	
Unit cell dimensions	a = 19.6993(3) Å	α= 90°.
	b = 13.7805(2) Å	β= 92.071(2)°.
	c = 17.3821(3) Å	γ = 90°.
Volume	4715.57(13) $Å^3$	
Z	4	

Density (calculated)	1.252 Mg/m^3
Absorption coefficient	0.686 mm^{-1}
F(000)	1840
Crystal size	0.285 x 0.184 x 0.054 mm^3
Theta range for data collection	2.244 to 75.519 °.
Index ranges	-22<=h<=24, -17<=k<=16,
-20<=l<=21	
Reflections collected	33472
Independent reflections	9395 [R(int) = 0.0201]
Completeness to theta = 67.679 °	99.7 %
Absorption correction	Semi-empirical from equivalents
Max. and min. transmission	1.000 and 0.60295
Refinement method	Full-matrix least-squares on F^2
Data / restraints / parameters	9395 / 1 / 613
Goodness-of-fit on F^2	1.069
Final R indices [I>2sigma(I)]	R1 = 0.0644, wR2 = 0.1927
R indices (all data)	R1 = 0.0821, wR2 = 0.2088
Extinction coefficient	n/a
Largest diff. peak and hole	0.184 and -0.141 $e.Å^{-3}$

8. References

1. G. Xie , X. Li , D. Chen , Z. Wang , X. Cai , D. Chen , Y. Li , K. Liu , Y. Cao and S.-J. Su, *Adv. Mater.*, 2016, **28**, 181-187.

2. B. Li, Z. Li, T. Hu, Y. Zhang, Y. Wang, Y. Yi, F. Guo and L. Zhao, *J. Mater. Chem. C*, 2018, **6**, 2351-2359.

3. M. M. Rothmann, S. Haneder, E. D. Como, C. Lennartz, C. Schildknecht and P. Strohriegl, *Chem. Mater.*, 2010, **22**, 2403-2410.

4. M.-X. Wang and H.-B. Yang, *J. Am. Chem. Soc.*, 2004, **126**, 15412-15422.